Nuclear Engineering and Technology 53 (2021) 2646–2651

Contents lists available at ScienceDirect

Nuclear Engineering and Technology

journal homepage: www.elsevier.com/locate/net

Original Article

# Performance evaluation of an adjustable gantry PET (AGPET) for small animal PET imaging

Hankyeol Song [a], In Soo Kang [a], Kyu Bom Kim [b], Chanwoo Park [a], Min Kyu Baek [a], Seongyeon Lee [a], Yong Hyun Chung [a, *]

[a] Department of Radiation Convergence Engineering, Yonsei University, Wonju, South Korea
[b] Department of Integrative Medicine, Major in Digital Healthcare, Yonsei University, Seoul, South Korea

ARTICLE INFO

*Article history:*
Received 15 November 2020
Received in revised form
29 December 2020
Accepted 30 January 2021
Available online 3 February 2021

*Keywords:*
Small animal PET
Adjustable gantry
DOI
Pulse reconstruction

ABSTRACT

A rectangular-shaped PET system with an adjustable gantry (AGPET) has been developed for imaging small animals. The AGPET system employs a new depth of interaction (DOI) method using a depth dependent reflector patterns and a new digital time pickoff method based on the pulse reconstruction method. To evaluate the performance of the AGPET, timing resolution, intrinsic spatial resolution and point source images were acquired. The timing resolution and intrinsic spatial resolution were measured using two detector modules and Na-22 gamma source. The PET images were acquired in two field of view (FOV) sizes, 30 mm and 90 mm, to demonstrate the characteristic of the AGPET. As a result of in the experiment results, the timing resolution was 0.9 ns using the pulse reconstruction method based on the bi-exponential model. The intrinsic spatial resolution was an average of 1.7 mm and the spatial resolution of PET images after DOI correction was 2.08 mm and 2.25 mm at the centers of 30 mm and 90 mm FOV, respectively. The results show that the proposed AGPET system provided higher sensitivity and resolution for small animal imaging.


## 1. Introduction

Positron Emission Tomography (PET) for preclinical imaging is a very useful instrument and has been used in a wide range of fields such as disease detection, staging and classification [1]. Especially, small animal PET is a non-invasive method, helping in the study and effective treatment of certain diseases. In conventional small animal PET systems, the system is designed to form a cylindrical gantry in which small detector modules are arranged in a circle and has sufficient field of view (FOV) to handle objects of various sizes [2]. However, by arranging the detector modules in a circle, coincidence events can escape through the gaps between detector modules in circular scanner [3]. In addition, when measuring objects smaller than gantry size, the sensitivity is reduced by escaping coincidence counts through the empty space between the detector and the object [4]. In order to enhance this problem, PET systems using a rectangular gantry have been developed [5–7], but a parallax errors also occur in a rectangular gantry, which degrades the spatial resolution of the system as the source moves to the outward FOV [8]. Depth of interaction (DOI) information is an important factor in reducing parallax errors and helps to provide uniform spatial resolution within the FOV. Also, improved sensitivity can be achieved by using an adjustable detector ring size, which increases the solid angle coverage [9].

In previous study, we proposed an adjustable gantry PET (AGPET) system with a rectangular gantry that can modify the FOV size [10]. Also, a new DOI method based on depth dependent reflector patterns [11,12] and a digital time pick-off method using a pulse reconstruction algorithm based on a bi-exponential model were developed to improve spatial and timing resolution, respectively [13].

In this study, the AGPET system was implemented and the system performances such as spatial resolution and timing resolution, were evaluated. PET images were acquired at two different FOV

* Corresponding author. Department of Radiation Convergence Engineering, College of Health Science, Yonsei University, Heungup, Wonju, Gangwondo, 220-710, South Korea.
*E-mail address:* ychung@yonsei.ac.kr (Y.H. Chung).

https://doi.org/10.1016/j.net.2021.01.037

sizes, 30 mm and 90 mm gantries with and without DOI correction. Spatial resolution was obtained experimentally at various source positions and compared with GATE simulation results.

## 2. Materials and methods

### 2.1. Detector assembly and DOI method

The AGPET detector module consists of an array of 12 × 12 polished LYSO crystals optically coupled to an 8 × 8 SiPM array (ArrayJ 30035–64P, SensL). The LYSO crystal (LYSO, EPIC Crystal Inc.) has a cross section of 2.1 × 2.1 $mm^2$ and a height of 20 mm. In the detector block, two detector modules were arranged in a 1 × 2 array coupled with an anger signal processing board. Anger logic circuit (AB4L-ArrayJ64p-2X1-SL64, AiT Instruments) converts 128 channels of SiPM signal into 4 channels of anger logic position information to form one detector block. Fig. 1 shows the LYSO array and detector module configuration [10].

Reflector patterns for two-layer DOI identification were applied to each detector module as shown in Fig. 2. Diffuse reflective paint (BC-620, Saint-Gobain) was used to paint the front and back layers 6 mm and 14 mm high, respectively [12]. The reflector paint was spread approximately 100 μm thick.

### 2.2. Data acquisition setup

Fig. 3 shows a schematic diagram of the AGPET structure consisting of 4 detector heads, each with 2 detector blocks, placed on a rectangular gantry adjustable in size from 30 mm to 90 mm. The 128 output signals were multiplexed into 4 position signals at each detector head. The position signals were fed to a signal processing board that generates the differential signal which is the positive and negative signal of the input signal. The differential signals were sent to the ADC on a dedicated DAQ system based on a free-running FPGA. In the experimental setup, DAQ used 8 ADC chips with 12-bit resolution and 65 MSPS speed to sample a total of 64 signals simultaneously, and SDRAM and a high-speed USB chip to free up data storage space.

The output signal from the detector head has a pulse length of 350 ns and the free-running ADC system operates at a 65 MHz sampling rate. A total of 21 samples were collected to obtain a complete pulse shape. On the FPGA, the module number, energy, time and position information were recorded in the data packet. In the data packet, the time information was stored as the clock sequence of the first sample of the pulse. For coincidence event sorting, the pulse start time was extracted using a pulse reconstruction method based on bi-exponential curve fitting [14]. Equation (1) shows the formula for the bi-exponential curve fitting.

$$y(t) = A \times exp\left(-\frac{t-t_0}{b}\right) \times \left[1 - exp\left(-\frac{t-t_0}{d}\right)\right] \quad (1)$$

where A is the amplification factor, $t_0$ is the pulse start time, b is the pulse rise time and d is the pulse decay time. For the curve fitting model, we used MATLAB software to set up a custom curve fitting algorithm and set $t_0$ as the output variable of the curve fitting.

### 2.3. System performance measurement

A flood map histogram for the detector module was acquired using a 10 μCi Na-22 source placed 10 cm from the detector surface. The temperature fluctuation was not considered but the experiment was conducted while maintaining the environment at 10 °C. Using the histogram, a lookup table was created to identify the segments of each crystal pixel, and 144 energy spectra were derived for each pixel. To measure timing resolution, two detector modules were built and a Na-22 source was placed at the center of the two detector modules. Then, the pulse start time was determined by the pulse reconstruction method and the difference between the two pulse start times was plotted as a time spectrum. The timing resolution was determined by the FWHM of the time spectrum.

After calculating the timing resolution, the intrinsic spatial resolution was measured with two detector modules and a Na-22 point source. The source was initially placed in the center of the two detector modules and moved radially at intervals of 0.3 mm. Then, the number of coincidence counts reaching two opposite pixels was recorded at each source location to get coincidence point spreads function (PSF). Fig. 4 illustrates the schematic diagram of the experimental setup for measuring intrinsic spatial resolution.

Point source images were acquired to evaluate the spatial resolution of the AGPET system. To take into account the characteristics of the AGPET system, PET images were obtained on two different gantry sizes, 30 mm and 90 mm. In the 30 mm AGPET, the source was placed at positions of 0, 5 and 10 mm from the center of the FOV. In the 90 mm AGPET, the source was located at 0, 10, 20, 30 and 40 mm from the center of the FOV. For 2D image reconstruction, the axial information was compressed into a central single slice through the single slice rebinning (SSRB) and a filtered back projection (FBP) algorithm with ram-lak filter was applied. Reconstructed images were acquired with or without DOI correction to evaluate the proposed DOI method. The timing window was set to 5 ns and energy window was from 450 keV to 650 keV. A 10 μCi Na-22 source was placed on a rotating stage and the source was rotated at 20° per 10 min. Fig. 5 shows the experiment setup for the spatial resolution measurement.

Spatial resolution was evaluated with the line profile of the point source image at each location and the FWHM of the Gaussian

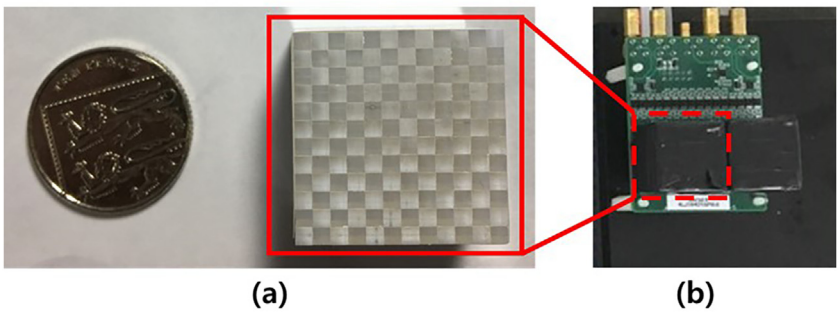


**Fig. 1.** Detector assemblies, (a) 12 × 12 LYSO module, (b) Detector block consisting of two detector modules and an Anger board.

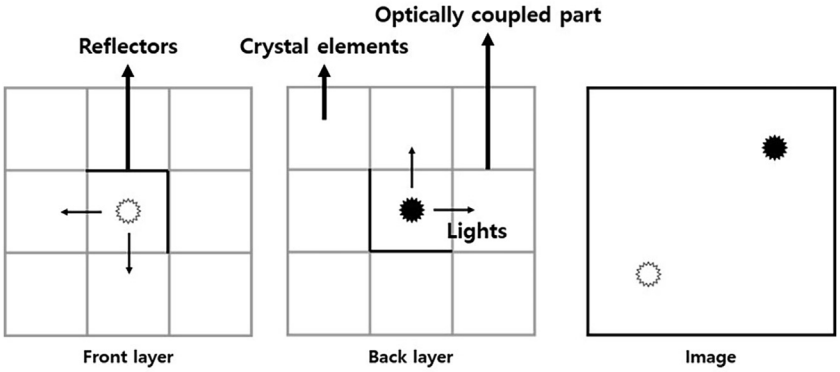


**Fig. 2.** Depth dependent reflector pattern for two layers of DOI measurement.

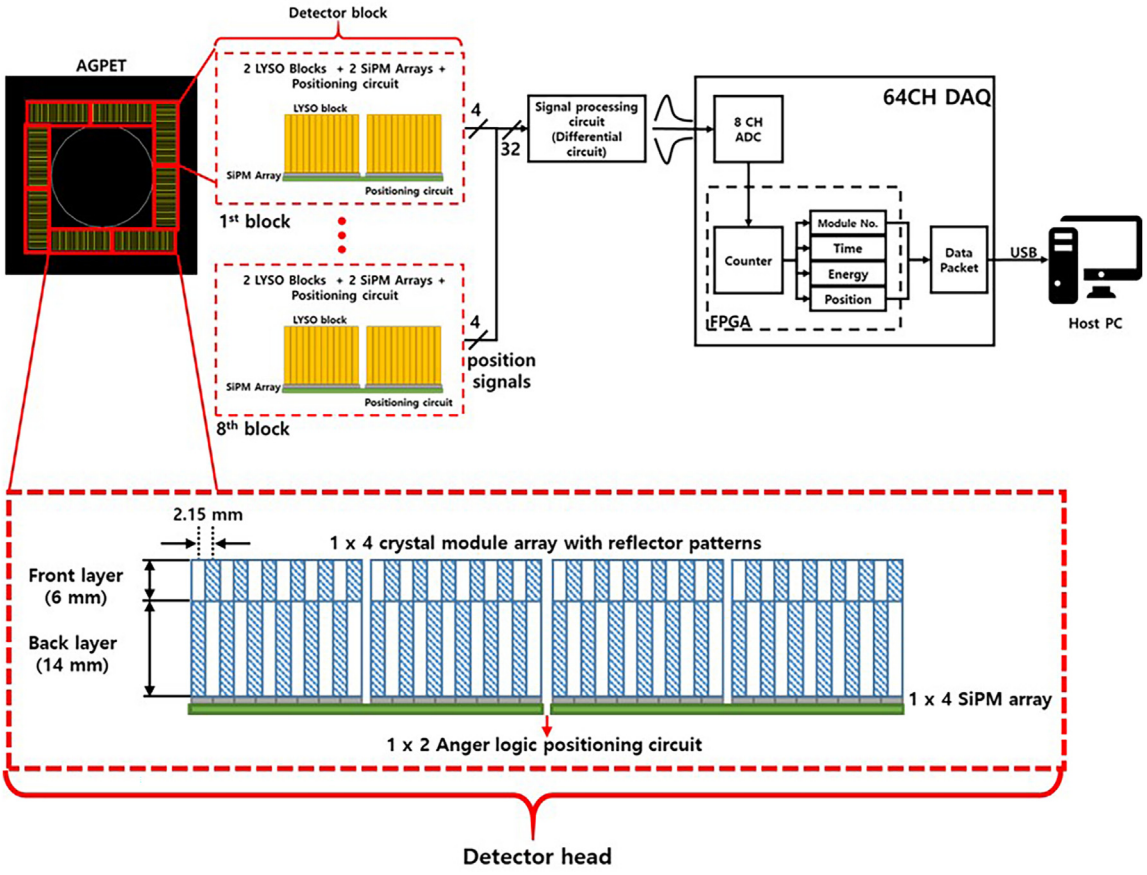


**Fig. 3.** Structure of the detector configuration for AGPET system and data acquisition process.

fit curve was obtained for the line profile. The spatial resolution obtained through the experiment was compared with GATE simulation results obtained in previous studies [10].

## 3. Results

Fig. 6 shows 2D flood histograms for the two detector modules and Fig. 7 shows the timing resolution spectrum of the AGPET detector. The timing resolution was calculated by the pulse reconstruction method and was 0.9 ns?

Fig. 8 illustrates the intrinsic spatial resolution profiles of two AGPET detectors measured across 12 crystal pairs along the radial direction in the FOV. The average intrinsic spatial resolution was 1.7 mm.

Fig. 9 shows Na-22 point source images at 3 different positions with and without DOI correction with 30 mm FOV of the AGPET system by FBP reconstruction. Fig. 10 shows the spatial resolution from experiments and simulations as a function of source offset. Before DOI correction, the spatial resolution was from 2.1 mm to 2.7 mm depending on the source offset. After DOI correction, the spatial resolution has been improved to a range of 2.0 mm–2.4 mm.

Fig. 11 shows the point source images at 5 different positions with and without DOI correction with 90 mm FOV of the AGPET system. Fig. 12 shows the spatial resolution from experiments and simulations as a function of source offset. Before DOI correction, the spatial resolution was from 3.0 mm to 6.5 mm. After the DOI

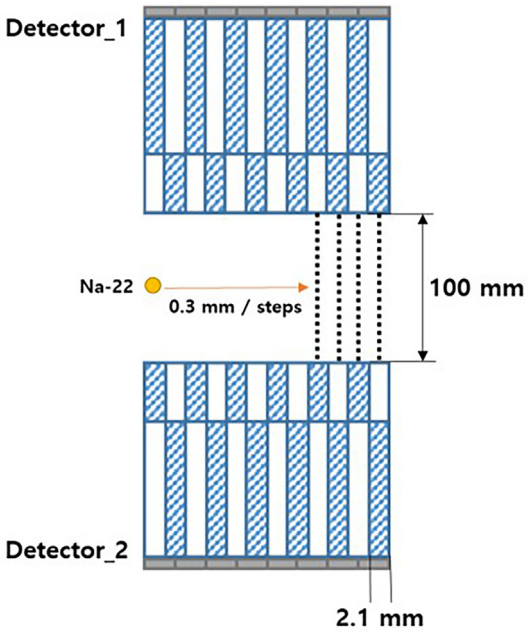


**Fig. 4.** Schematic diagram of the experimental setup for measuring intrinsic spatial resolution.

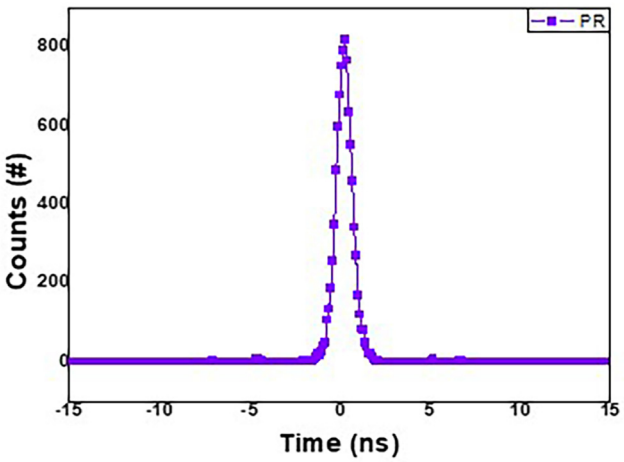


**Fig. 7.** Timing resolution spectrum of two detector module (0.9 ns)

correction, the spatial resolution has been significantly improved to ~3.0 mm. The experiment results were also consistent with the GATE simulation results.

## 4. Discussion and conclusion

The AGPET system was developed and performance was evaluated. The AGPET employed the adjustable rectangular gantry and a

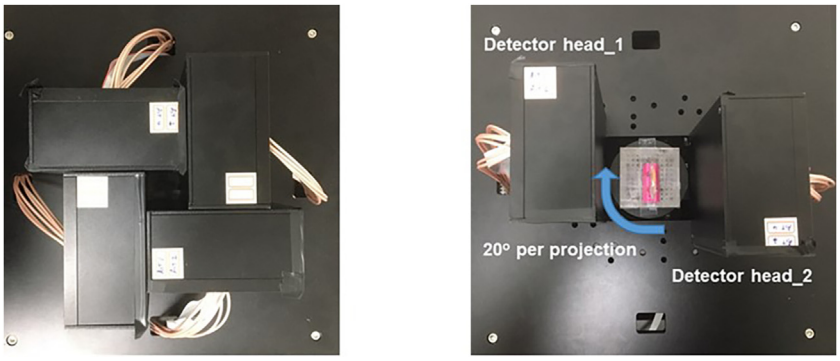


**Fig. 5.** Experiment setup for PET image acquisition using two and four detector heads.

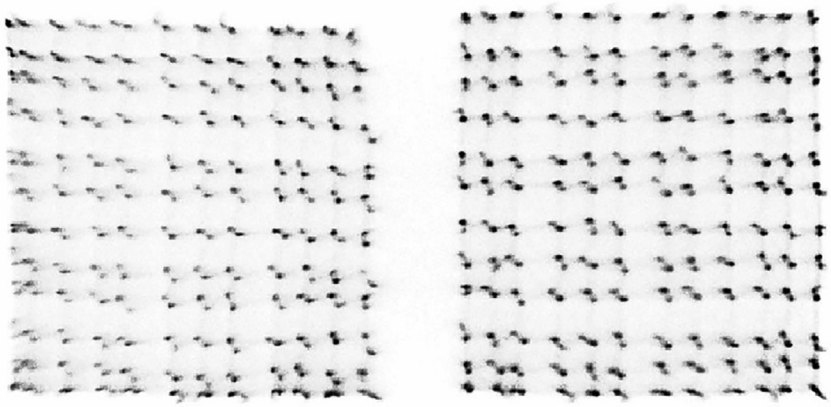

**Fig. 6.** 2D flood histograms of the detector modules.

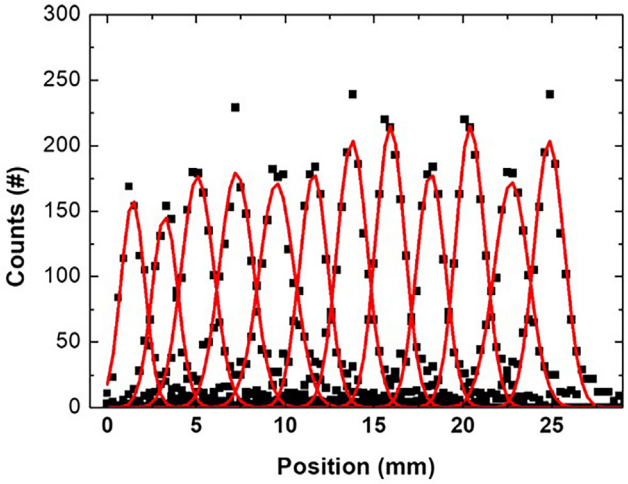


**Fig. 8.** Intrinsic spatial resolution using two detector module.

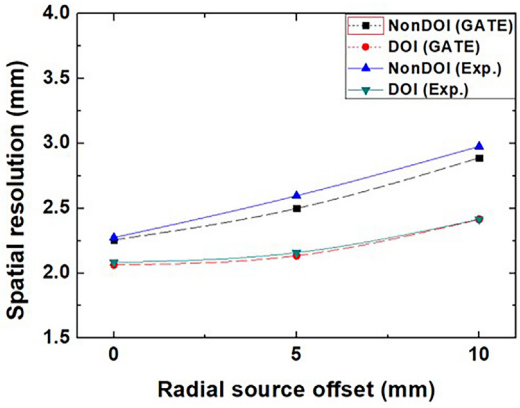


**Fig. 10.** Spatial resolution obtained through experiments and simulations with and without DOI correction.

new DOI method based on the depth dependent reflector patterns. In addition, a new digital time pickoff method was applied to compensate for relatively slow DAQ devices. System performance was evaluated in terms of timing resolution, intrinsic spatial resolution and system spatial resolution. In the previous study, digital timing pickoff algorithm was compared with various timing resolution measurement method. As a result, timing pickoff method was useful for improving timing resolution. The timing resolution was 1.4 ns calculated by the initial rising interpolation method. The timing resolution was improved to 0.9 ns using the pulse reconstruction method. The better timing resolution allows to set a narrow timing window of PET system and the narrow timing window rejects random coincidence events, contributing to improving system performance in sensitivity and spatial resolution. An average of 1.7 mm intrinsic spatial resolution was measured. The crystal elements of the AGPET detector had a cross-sectional area of $2.1 \times 2.1$ mm$^2$ and the results demonstrate that the detector can clearly resolve all crystal elements. The spatial resolution of the point source image was 2.08 mm and 2.25 mm at the center of the 30 mm and 90 mm FOV, respectively. Before the DOI correction, the spatial resolution was degraded by parallax error at the periphery region of the FOV. However, after DOI correction, the spatial resolution was improved by compensating the parallax error. In particular, the spatial resolution was significantly improved at the outskirt of the FOV and the results show that the proposed DOI method contributes to the parallax error compensation.

Based on system performance evaluation, the AGPET has been proven to provide high resolution by applying the DOI measurement and to provide high sensitivity by modifying the FOV to fit the object size. In addition, a digital time pick-off method based on pulse reconstruction can contribute to better sensitivity and resolution. In this study, the sensitivity and effect of timing resolution were not quantitatively evaluated, but in future studies, the factors will be evaluated through NECR (Noise Equivalent Count Rate) measurement and phantom image study. In addition, gap compensation is required to compensate for artifacts caused by gaps between detector heads.

The AGPET system has the potential to provide higher sensitivity

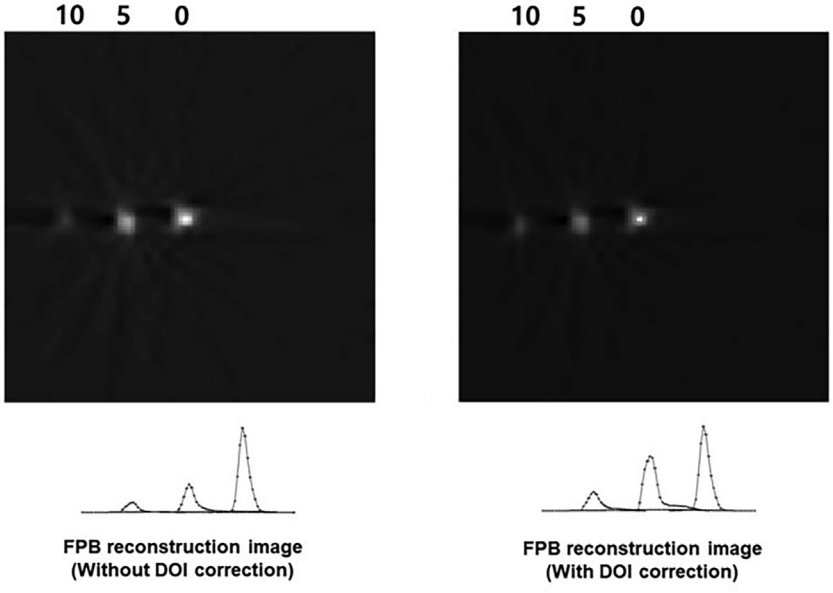


**Fig. 9.** Na-22 point source images without (left) and with (right) DOI correction (FOV: 30 mm).

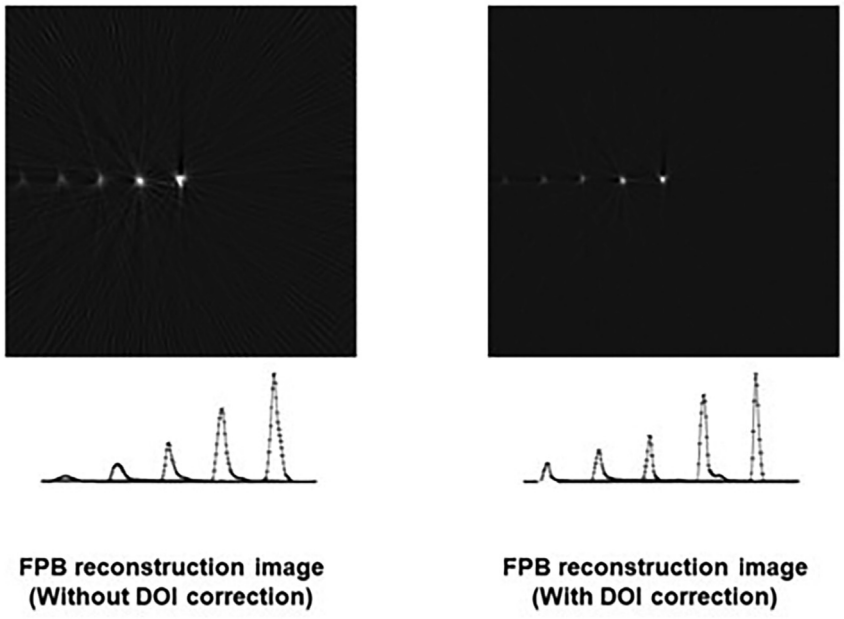


**Fig. 11.** Na-22 point source images without (left) and with (right) DOI correction (FOV: 90 mm).

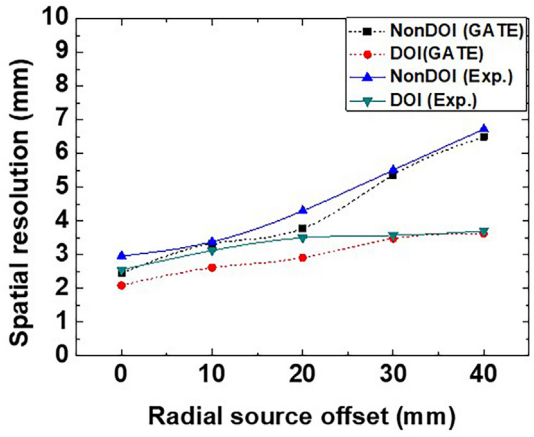


**Fig. 12.** Spatial resolution obtained through experiments and simulations with and without DOI correction.

and spatial resolution for small animal imaging and its quantitative evaluation will be reported in further studies.

## Declaration of competing interest

The authors declare that they have no known competing financial interests or personal relationships that could have appeared to influence the work reported in this paper.

## Acknowledgement

This work was supported by the Nuclear Safety Research Program through the Korea Foundation Of Nuclear Safety (KoFONS) using the financial resource granted by the Nuclear Safety and Security Commission (NSSC) of the Republic of Korea No. 1903013.

## References

[1] Juan José Vaquero, Kinahan Paul, Positron emission tomography: current challenges and opportunities for technological advances in clinical and preclinical imaging systems, Biomed. Eng. 17 (2015) 385–414.
[2] H. Zhang, Q. Bao, N.T. Vu, R.W. Silverman, R. Taschereau, B.N. Berry-Pusey, A. Douraghy, F.R. Rannou, D.B. Stout, A.F. Chatziioannou, Performance evaluation of PETbox: a low cost bench top preclinical PET scanner, Mol. Imag. Biol. 13 (2011) 949–961.
[3] F. Habte, A.M.K. Foudray, P.D. Olcott, C.S. Levin, Effects of system geometry and other physical factors on photon sensitivity of high-resolution positron emission tomography, Phys. Med. Biol. 52 (2007) 3753–3772.
[4] R.S. Miyaoka, T.K. Lewellen, H. Yu, D.L. McDaniel, Design of a depth of interaction (DOI) PET detector module, IEEE Trans. Nucl. Sci. 45 (1998) 1069–1073.
[5] S. España, R. Marcinkowski, V. Keereman, S. Vandenberghe, R. Van Holen, DigiPET: sub-millimeter spatial resolution small-animal PET imaging using thin monolithic scintillators, Phys. Med. Biol. 59 (2014) 3405–3420.
[6] Z. Gu, R. Taschereau, N.T. Vu, H. Wang, D.L. Prout, R.W. Silverman, B. Bai, D.B. Stout, M.E. Phelps, A.F. Chatziioannou, NEMA NU-4 performance evaluation of PETbox4, a high sensitivity dedicated PET preclinical tomograph, Phys. Med. Biol. 58 (2013) 3791–3814.
[7] Z. Gu, R. Taschereau, N. Vu, H. Wang, D. Prout, R. Silverman, D. Stout, M. Phelps, A. Chatziioannou, Design and Initial Performance of PETbox4, a High Sensitivity Preclinical Imaging Tomograph, 2011, IEEE Nuclear Science Symposium Conference Record, 2011, pp. 2328–2331.
[8] K. Chien-Min, P. Xiaochuan, C. Chin-Tu, Accurate image reconstruction using DOI information and its implications for the development of compact PET systems, IEEE Trans. Nucl. Sci. 47 (2000) 1551–1560.
[9] Xin Li, Maria Ruiz-Gonzalez, Lars R. Furenlid, An edge-readout, multilayer detector for positron emission tomography, Med. Phys. 45 (2018) 2425–2438.
[10] H. Song, S.-J. Lee, C. Park, I.S. Kang, K.B. Kim, Y.H. Chung, Feasibility of adjustable-gantry PET system using advanced DOI method, Nucl. Instrum. Methods Phys. Res. Sect. A Accel. Spectrom. Detect. Assoc. Equip. 953 (2020) 163087.
[11] S.-J. Lee, C. Lee, Y.H. Chung, J. Kang, C.-H. Baek, Development of a novel depth-of-interaction encoding method and use of light spreading in a scintillation crystal array with single-ended readout, J. Kor. Phys. Soc. 69 (2016) 1842–1846.
[12] S.-J. Lee, C. Lee, J. Kang, Y.H. Chung, A new DOI detector design using discrete crystal array with depth-dependent reflector patterns and single-ended readout, Nucl. Instrum. Methods Phys. Res. Sect. A Accel. Spectrom. Detect. Assoc. Equip. 843 (2017) 1–4.
[13] C.P. Hankyeol Song, Min Kyu Baek, Seongyeong Lee, Kyu Bom Kim, Yong Hyun Chung, Timing Pickoff Method for Improvement of Timing Resolution in AGPET, Nuclear Engineering and Technology, 2020.
[14] D. Xi, C. Kao, W. Liu, C. Zeng, X. Liu, Q. Xie, FPGA-only MVT digitizer for TOF PET, IEEE Trans. Nucl. Sci. 60 (2013) 3253–3261.